Biointerface Research in Applied Chemistry
Platinum Open Access Journal (ISSN: 2069-5837)

Article
Volume 11, Issue 4, 2021, 12186 - 12201
https://doi.org/10.33263/BRIAC114.1218612201

Plantago Major Extract as an Environmentally Friendly Inhibitor for the Corrosion of L-80 Carbon Steel in 0.5 M H_2SO_4 Media

Mohamed A. EL-Zekred [1], Abd El-Aziz S. Fouda [1], Ashraf M. Nofal [2], Kamal Shalabi [1,*]

[1] Chemistry Department, Faculty of Science, Mansoura University, Mansoura, Egypt; Mohamed_ahmed902009@yahoo.com (M.A.E.-Z.); asfouda@hotmail.com (A.S.F.);
[2] Environmental Studies and Research Institute, University of Sadat City, Sadat City, Egypt; dr.ashrafnofal20@yahoo.com (A.M.N.);
* Correspondence: dr-kamal@mans.edu.eg;

Scopus Author ID 2666715790
Received: 3.12.2020; Revised: 29.12.2020; Accepted: 30.12.2020; Published: 3.01.2021

Abstract: The inhibition impact of Plantago major leaves extract on carbon steel (CS) which immersed in 0.5 M H_2SO_4 media was investigated by several methods such as mass loss method (ML), electrochemical impedance spectroscopy (EIS), potentiodynamic polarization (PDP), and electrochemical frequency modulation (EFM). Data obtained from different measurements was showed that %IE enhanced with added the Plantago major extract doses also increased with increasing temperature degree. Thermodynamic adsorption and kinetic parameters of the system were also measured and studied. The adsorption of the Plantago major extract on CS is, according to Temkin isotherm. The curves from PDP explained that the Plantago major extract is considered as a mixed-type inhibitor. The EIS technique's acquired data verified that the studied extract produced a thin layer that covers and protects the CS surface. Atomic Force Microscopy (AFM) and Fourier Transform Infrared (FT-IR) analysis conformed that Plantago major extract was adsorbed on CS surface. The data obtained from unlike measurements were in good accord.

Keywords: carbon steel; corrosion inhibition; H_2SO_4; Plantago; EIS; EFM; FT-IR; AFM.

1. Introduction

Studying metal corrosion and how to protect it from corrosion is extremely important due to the resulting problems, as the economic losses due to material degradation. Corrosion is the decomposition and dissolution of alloys and metals by electrochemical and chemical reactions with the surrounding environment [1]. CS is regarded as one of the most significant materials used for petroleum purposes, pipelines, tanks, ships, equipment, and other industries due to its excellent mechanical properties at high temperature, ease of manufacture, and its cost. However, it is prone to corrosion when it comes in contact with an acidic solution, scientific researchers are doing their best to solve this problem. Acidic solutions are used in industrial applications where sulfuric acid is the most used to remove oxides that are formed in the steel, oil refinery by chemical procedures [2-5]. Over time, the use of these acid solutions can damage metals. Inhibitors are materials that are added in small quantities to protect all metals and alloys from corrosion attack. One of the best protection methods is the green inhibitor, which has many advantages: low cost, safe environment, availability, and renewable resources. There are many types of research published on the employment of natural products

as corrosion protection [6-12]. Some of the plant extracts have been successfully proved for their effectiveness on the deterioration of CS in acidic environments [13-26]. The Plantago major has been utilized to treat some diseases and has bioactive agents for wound healing effects, anti-ulcerative, anti-diabetic, anti-diarrhoeal, anti-inflammatory, anti-cancer, anti-fatigue, antioxidant and free radical scavenger, anti-bacterial, and anti-viral [27]. In this investigation, we study the inhibition impact of Plantago major extract on the corrosion of CS with 0.5 M H_2SO_4. The techniques used for this study were ML and electrochemical tests. The adsorption of Plantago major extract on the CS surface has been proved by Atomic Force Microscopy (AFM) and Fourier Transform Infrared (FT-IR).

2. Materials and Methods

2.1. Composition of CS samples.

The CS samples used in the experiments are of L-80 CS type, which is: 0.040 %P, 0.050 %S, 0.15-0.20 %C, 0.60-0.90 %Mn, and Fe rest. This constitution, according to the American Iron and steel institute (AISE). The dimension of the specimens is 20 x 20 x 2 mm. Before starting measurements, the samples must be treated by unlike grades of emery paper, then washed with de-ionized water and dried with filter papers.

2.2. Preparation of corrosive media.

The destructive solution used in the study was 0.5 M H_2SO_4, which was prepared by diluted analytical reagent grade H_2SO_4 by de-ionized water.

2.3. Preparation of plant extracts.

After collecting Plantago major leaves, we dried them at room temperature and ground them into a fine powder by using an electrical mill. Take about two hundred grams (200g) of this powder and soaked into 800 ml of methanol at a ratio of 1:4 (powder/solvent). Under vacuum, the extract was isolated then dried by rotary evaporator [28]. The investigated extract was liquefied in ethanol (1g/L) and stored in the refrigerator. Fourier Transform Infrared (FT-IR) technique was used to recognize functional groups that existed in Plantago major extract before and next study of the corrosion inhibition. There are various bioactive compounds found in Plantago major extract: Carbohydrates, Lipids, Alkaloids, Caffeic acid, Flavonoids, Iridoid glycosides, and other terpenoids [29].

2.4. Chemical technique (ML method).

At first, the CS specimens must be physically treated before starting the study using emery papers of unlike grades abraded to finish a mirror then washed by bi-distilled water and desiccated by filter papers. Samples were weighted by electrical balance. The doses used of Plantago major extract was varied from 50 to 300 ppm. The coupons were dipped into a solution of 100 ml of 0.5 M of H_2SO_4 in the lack and existence of unlike Plantago major extract doses for 180 min. The immersion time is 30 min, where the samples were weighed again. The rates of corrosion (CR), the surface coverage (θ), and the inhibition efficiency ($\%IE_{ML}$) obtained from the ML method were reckoned from the following equations. [30,31]:

$$CR = \frac{M}{At} \quad (1)$$

$$\theta = \frac{CR - CR_{(i)}}{CR} \quad (2)$$

$$\%IE_{ML} = \theta \times 100 \quad (3)$$

where "M = reduction in mass (mg), $CR_{(i)}$ and CR are the rate of corrosion with and without extract, respectively, t is the immersion time (min), and A is the area of the surface (cm^2)".

2.5. Electrochemical technique.

Three different electrodes are placed together in a glass cell for electrochemical measurements. A reference electrode is $Ag/AgCl_{(s)}$ electrode, the platinum wire is an auxiliary electrode, and the working electrode is made from CS with an exterior area 10 mm^2. The working electrode surface must be physically treated in the same approach as ML method [32]. Before starting a measurement, CS electrode was placed in the studied solution for 20 min to attain a steady-state (OCP). For potentiodynamic polarization tests, the applied potential was from -0.5 to + 0.5 V at (OCP) with scan rate 1 mVs^{-1}. The current of corrosion i_{corr} was evaluated from the extrapolating of anodic and cathodic (β_a & β_c) Tafel slopes to obtain i_{corr}, to measure IE% of the inhibitor and (θ) we used the following relation:

$$\%IE_{PDP} = [\,1 - \frac{i_{corr(inh)}}{i_{corr(free)}}] \times 100 \quad (4)$$

wherever "$i_{corr\ (free)}$ and $i_{corr\ (inh)}$ are the current densities for without and with inhibitors"correspondingly. The impedance tests (EIS) were done with a frequency variety of 100 kHz to 0.2 Hz peak-to-peak amplitude of 10 mV at (OCP). The %IE is calculated from this formula:

$$\%IE_{EIS} = [\,1 - \frac{R_{ct(free)}}{R_{ct(inhi)}}] \times 100 \quad (5)$$

wherever "$R_{ct\ (free)}$ and $R_{ct\ (inh)}$ are the resistances of charge transfer for nonexistence and existence of inhibitors," respectively. For EFM measurements, we utilized two frequencies of range 2 and 5 Hz [33-35]. The corrosion current, Causality factors (CF-2, CF-3), and β_a & β_c Tafel slopes were evaluated using the biggest peeks.

2.6. Examination of the Surface by AFM, FT-IR.

The CS specimens understudied were immersed in a solution of 0.5 M of H_2SO_4 in the lack and the existence of 300 ppm of Plantago major extract. The coupons were removed after 24 h and let in the air dry at room temperature; then, the morphological surface of the studied CS specimens was examined by Atomic force microscopy (AFM). The film formed on CS surface was examined by Fourier transforms infrared spectroscopy with a varied wave number from 400 – 4500 cm^{-1}.

3. Results and Discussion

3.1. Mass loss (ML) measurements.

3.1.1. Effect of concentration and temperature.

The CR of studied CS was determined before and after added different doses of Plantago major extract by calculating the ML per area per unit time. CS samples' mass measured before and after immersion time for 180 min in the uninhibited and inhibited corrosive solution by electrical balance. ML curves against time at 25 °C for CS in 0.5 M H_2SO_4 before and after adding unlike doses of Plantago major extract was shown in Fig.1**.** ML

measurements were done at various temperatures of 25, 35, 45, and 55 ˚C. The impact of temperature on the CR of CS in the lack and existence of diverse concentrations of Plantago major extract was shown in Table 1. From the data in this table, we noticed that the CR was diminished with the investigated inhibitor's rising concentration, so the %IE increases. This occurs by the adsorption of Plantago major extract on the CS surface and by rising the dose of the Plantago major plant extract lead to rising the surface coverage (θ) of the extract on the CS surface and forming a layer of the studied extract on CS which protect it from destroyed [36,37]. By increasing the temperature, the CR decreases, and the %IE of the Plantago major plant extract increasing, as shown in Table 1.

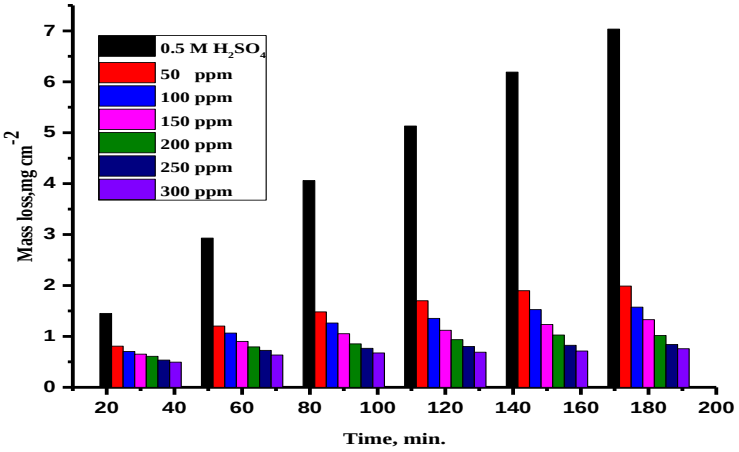

Figure 1. ML – time curves in the lack and existence unlike doses of Plantago major extract at 25.0˚C.

Table 1. Effect of unlike doses of Plantago major on CR and IE % of CS in H_2SO_4 (0.5 M) at unlike temperatures.

Inhi.	Conc., M	25.0˚C		35.0˚C		45.0˚C		55.0˚C	
		CR×10^{-2} mg cm^{-2} min^{-1}	%IE	CR×10^{-2} mg cm^{-2} min^{-1}	%IE	CR×10^{-2} mg cm^{-2} min^{-1}	%IE	CR×10^{-2} mg cm^{-2} min^{-1}	%IE
Plantago major	0.5 M H_2SO_4	4.276	_	10.853	_	25.387	_	39.992	_
	50	14.17	66.8	25.23	76.8	50.57	80.1	71.38	82.2
	100	11.29	73.6	18.76	82.7	34.97	86.2	51.52	87.1
	150	9.34	78.2	15.33	85.9	29.55	88.4	40.18	90.0
	200	7.80	81.8	12.19	88.7	24.10	90.5	30.78	92.3
	250	6.68	84.4	9.66	91.1	17.63	93.1	26.75	93.3
	300	5.75	86.5	7.27	93.3	15.03	94.1	20.10	94.9

3.2. Adsorption isotherms.

Several isotherm models were evaluated to examine the interaction between Plantago major extract and the CS surface. The Temkin isotherm was the appropriate model to illustrate the adsorption process. The expression of Temken model is:

$$\theta = \frac{2.303}{a} log\, K + \frac{2.303}{a} log\, C \qquad (6)$$

where "θ is the surface coverage, a is the parameter of molecular interaction, K is the equilibrium constant of adsorption, and C is the concentration of inhibitor". By plotting θ with log C Fig. 2, straight lines were acquired with intercept = 2.303/a log K and slope of lines =2.303/a.

The K_{ads} is related with the Gibbs free energy ($-\Delta G^{\circ}_{ads}$) by this formula:

$$log\, K_{ads} = -log\, 55.5 - \frac{\Delta G^{\circ}_{ads}}{2.303RT} \qquad (7)$$

where "R is the constant of universal gas, T is the absolute temperature, and the value of 55.5 is equal to water concentration".

Moreover, the enthalpy ΔH°_{ads} can be obtained from Van't Hoff equation (8) by plotting (log K_{ads}) versus (1/T) as demonstrated in Fig. 3.

$$\log K_{ads} = -\frac{\Delta H^{\circ}_{ads}}{2.303RT} + constant \quad (8)$$

The standard entropy ΔS°_{ads} parameter can be obtained in accordance with the following formula:

$$\Delta G^{\circ}_{ads} = \Delta H^{\circ}_{ads} - T\Delta S^{\circ}_{ads} \quad (9)$$

The data of thermodynamic parameters ($\Delta G^{\circ}_{ads.}$, $\Delta H^{\circ}_{ads.}$and $\Delta S^{\circ}_{ads.}$) and K_{ads} was recorded in Table 2 [38-40].

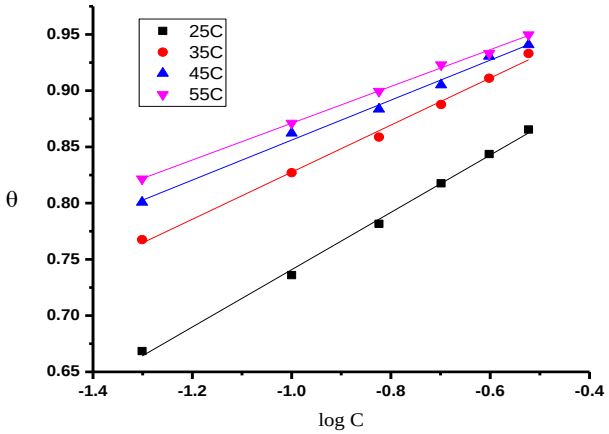

Figure 2. Temkin adsorption of Plantago major on the CS of at different temperatures.

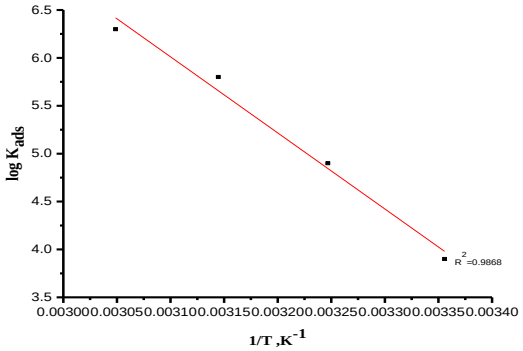

Figure 3. (1/T against log K_{ads}) curves existence and nonexistence of unlike doses of Plantago major extract.

Table 2. Data of thermodynamic adsorption parameters.

Inhibitor	Temp. K	$K_{ads.} \times 10^4$ mole^{-1}	$-\Delta G^{\circ}_{ads}$ kJ mol^{-1}	ΔH°_{ads} kJ mol^{-1}	ΔS°_{ads} J mol^{-1} k^{-1}
Plantago major	298	0.81	32.2	152.1	618.6
	308	8.9	39.5		622.0
	318	65.6	46.0		623.1
	328	212.0	50.6		618.1

From the data of thermodynamic adsorption parameters found in Table 2, the following notes can be written:

1- The negative sign of ($\Delta G^{\circ}_{ads.}$) indicated that the Plantago major extract is spontaneously absorbed on the surface of metal [41].

2- The results of $\Delta G^{\circ}_{ads.}$ are negative approximately - 40 kJ $mol^{-1,}$ which is affiliated with the chemical absorption reaction resulting from the transfer of electrons from the extract components to the empty d orbitals on the surface of the CS to form a coordination bond [42].
3- The positive data of $\Delta H^{\circ}_{ads.}$ indicated that the adsorption of Plantago major extract to CS occurs via an endothermic reaction associated with chemical absorption reaction [43].

3.3. Activation parameters.

The thermodynamic parameters of the destructive reaction's excitation state were evaluated from ML measurements at different temperatures. The activation energies (E_a^*) of the corrosion process were given from Arrhenius expression as follows [44]:

$$\log k_{corr} = \left(\frac{-E_a^*}{2.303RT}\right) + \log A \quad (10)$$

Where "E_a^* is the energy of activation, A is the factor of Arrhenius pre-exponential, and k_{corr} is the CR"obtained from ML measurements. Fig.4. showed (log k_{corr}) versus (1/T) for Plantago major extract, and straight lines were acquired.

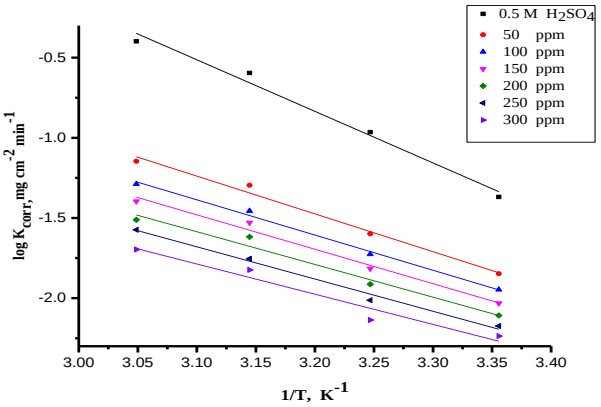

Figure 4. 1/T versus k_{corr} for existence and nonexistence of unlike doses of Plantago major extract.

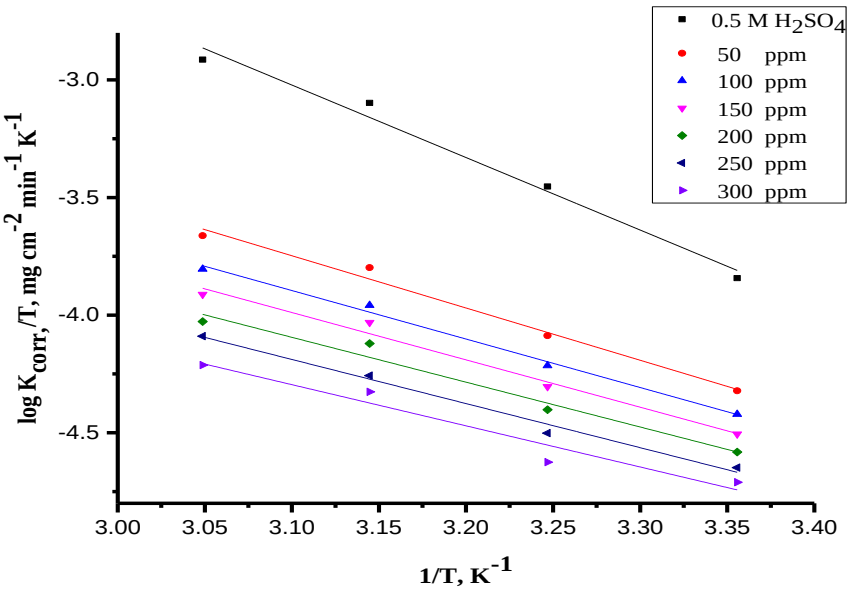

Figure 5. (1/T) against log (k_{corr}/T) curves in existence and nonexistence of unlike doses of Plantago major extract.

The obtained data of E_a^* was recorded in Table 3; with rising the Plantago major extract dose, the E^*_a values decreased, which indicates chemisorption adsorption [45,46]. The

activation entropy ΔS^* and activation enthalpy ΔH^* were estimated by transition state equation [47,48]:

$$\log k_{corr} = \log\left(\frac{R}{Nh}\right) + \frac{\Delta S^*}{2.303R} + \frac{\Delta H^*}{2.303RT} \quad (11)$$

Where "N is Avogadro's number, h is Planck's constant, ΔH^* is the enthalpy of activation, and ΔS^* is the activation entropy". Fig.5 displayed (log k_{corr} /T) against (1/T) for Plantago major extract. We can determine the activation parameters from values of slope and intercept of straight lines. The obtained values of activation parameters were recorded in Table 3. The positive sign of ΔH^* indicates the endothermic reaction of the dissolution process of CS [49]. The data of ΔS^* increment with increasing the dose of inhibitor, which is evidence for the formation of an activated [inhibitor-metal complex] in the rate-determining step [50,51]. The negative symbol of ΔS^* indicated that the activated [inhibitor-metal] prefersassociation instead of dissociation.

Table 3. Parameters for activation of CS in the lack and existence of different Plantago major extract concentrations in 0.5M H_2SO_4.

Inhibitor	Conc. M	Ea^* kJ mol^{-1}	ΔH^* kJ mol^{-1}	$-\Delta S^*$ J mol^{-1} K^{-1}
Plantago major	0.5 M H_2SO_4	61.6	25.6	72.5
	50	45.1	18.5	137.1
	100	42.1	17.1	149.8
	150	41.1	16.7	154.5
	200	39.1	15.8	162.8
	250	38.5	15.6	166.5
	300	36.1	14.5	176.0

3.4. Electrochemical measurements.

3.4.1. PDP measurements.

Tafel polarization curves of CS in 0.5M H_2SO_4 media before and after treating with unlike doses of Plantago major extract at 25°C was showed in Fig.6. The figure showed that the current densities of anodic and cathodic branches decrease by adding different concentrations of Plantago major extract, indicating the anodic and cathodic reactions were inhibited by plant extract. The electrochemical parameters E_{corr}, β_a & β_c, θ, IE %, and i_{corr} were estimated and established in Table 4.

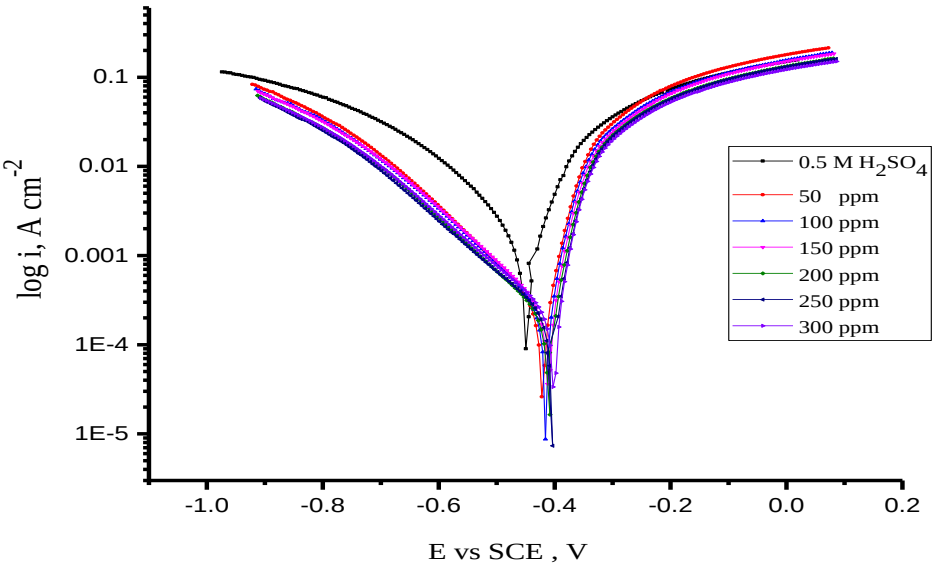

Figure 6. PDP plots for CS in the lack and existence of unlike doses of Plantago major at 25°C.

The acquired data showed that the current of corrosion (i_{corr}) was decreased by adding present extract leading to a decrease in the CR and increase of IE% owing to the establishment of a protective adsorbed layer of the plant extract. While the values of (E_{corr}) and (β_a& β_c) were not significantly changed, so the Plantago major extract performed as a mixed type of inhibitor, indicating that the Plantago major extract hindered both H_2 evolution process (cathodic reaction) and CS dissolution process (anodic reaction). Moreover, the non-significant change of β_a& β_c, revealing that the Plantago major extract does not modify the mechanism of CS corrosion in 0.5M H_2SO_4.

Table 4. electrochemical parameter, i_{corr}, E_{corr}, β_a, β_c, k_{corr}, θ and IE % of CS in 0.5M H_2SO_4 for existence and nonexistence unlike doses of Plantago major extract.

Inh.	conc., M	− E_{corr}, mV vs. SCE	β_a mV dec^{-1}	β_c mV dec^{-1}	i_{corr}, µA m^{-2}	θ	%IE_{PDP}
Plantago major	0.5 M H_2SO_4	449	106.0	188.4	1900	-	-
	50	421	110	200.0	479	0.748	74.8
	100	415	106	204.6	431	0.773	77.3
	150	411	83.7	199.5	394	0.793	79.3
	200	410	92.5	197.6	302	0.841	84.1
	250	404	73.0	192.0	243	0.872	87.2
	300	401	55.7	180.5	215	0.890	89.0

3.4.2. Electrochemical impedance (EIS) measurements.

The Nyquist and Bode plots of CS before and after adding different Plantago major extract doses are shown in Fig. (7-a) and (7-b), respectively. Nyquist plot shows one depressing capacitive loop, and Bode plot displays one phase angle maximum, which is attributed to the presence of one time constant in the corrosion process related to the electrical double layer existence in metal–solution interface [52]. The Fig. (7-a) curves showed a gradual rise in the shape of each semicircle of the Nyquist curves by raising the concentration of the present extract. The curves which result from Nyquist plots are not completely semicircle because of roughness and homogeneity of electrode surface [52].

In Fig.8, the equivalent circuit examined the EIS spectra for CS corrosion in 0.5M H_2SO_4 before and after adding Plantago major extract included R_s (solution resistance), R_{ct} (charge transfer resistance), and CPE_{dl} (constant phase element for a double layer). The following describes the impedance as a function of CPE [53]:

$$C_{dl} = Y_0 (\omega_{max})^{n-1} \quad (12)$$

where, "ω_{max} denotes the angular frequency when the imaginary component of the impedance at its maximum value, Y_0 is the magnitude of CPE, and n is a CPE exponent"relies on the character of the metal surface.

The %IE was estimated by using this Eq. [54]:

$$\%IE_{EIS} = \frac{R_{ct\,(inh)} - R_{ct}}{R_{ct\,(inh)}} \times 100 \quad (13)$$

where "R_{ct} is the resistance of charge transfer, and C_{dl} is the capacitance of double layer". The data of (IE %, θ, R_{ct}, and C_{dl}) are listed in Table 5. From acquired data, we are noted that there is an increase in (R_{ct}) by increasing Plantago major extract concentration, which demonstrates a rise in their protecting versus the corrosion by reason of the construction of adsorbed protective layer [55]. While the (C_{dl}) decreased owing to an increment in the electrical double layer thickness as the concentrations of Plantago major extract increased [56].

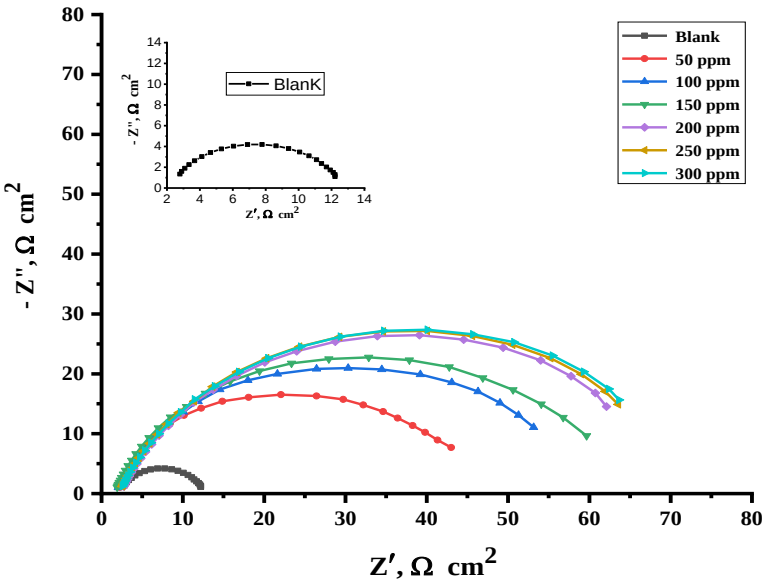

Figure 7-a. Nyquist curves for CS in the lack and existence of unlike doses of Plantago major extract.

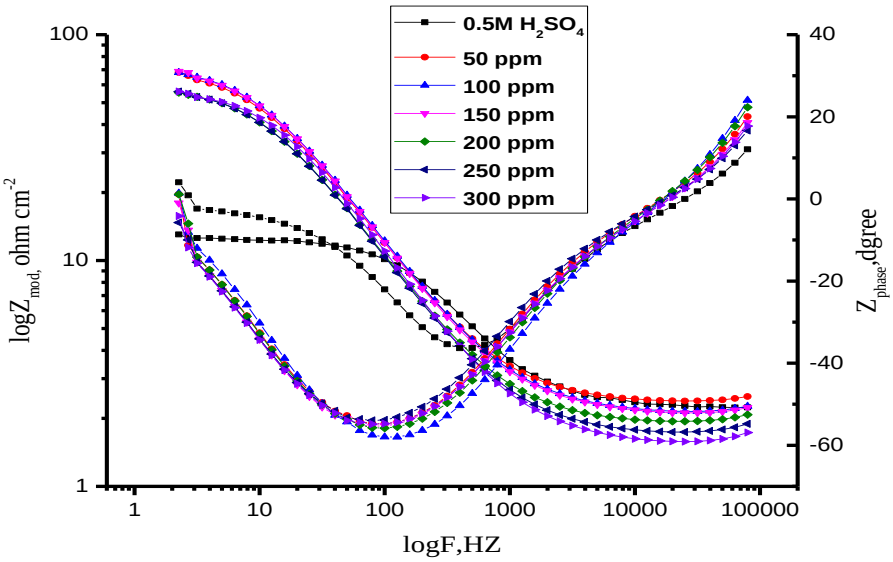

Figure 7-b. Bode curves for CS in 0.5M H_2SO_4 for existence and nonexistence of unlike doses of Plantago major extract.

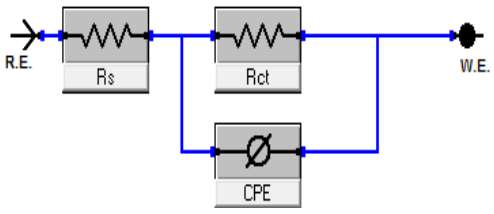

Figure 8. Equivalent circuit model.

Table 5. Data obtained from EIS measurements for CS corrosion in the lack and existence of unlike doses of Plantago major extract at 25˚C.

Inhibitor	Conc. M	R_{ct}, Ω cm²	C_{dl}, µF cm²	θ	%IE_{EIS}
Plantago major	0.5 M H_2SO_4	10.36	206.3	-	-
	50	40.85	192.4	0.746	74.6
	100	44.25	178.6	0.766	76.6
	150	46.00	173.4	0.775	77.5
	200	55.43	181.7	0.813	81.3
	250	57.05	177.8	0.818	81.8
	300	57.70	176.3	0.820	82.0

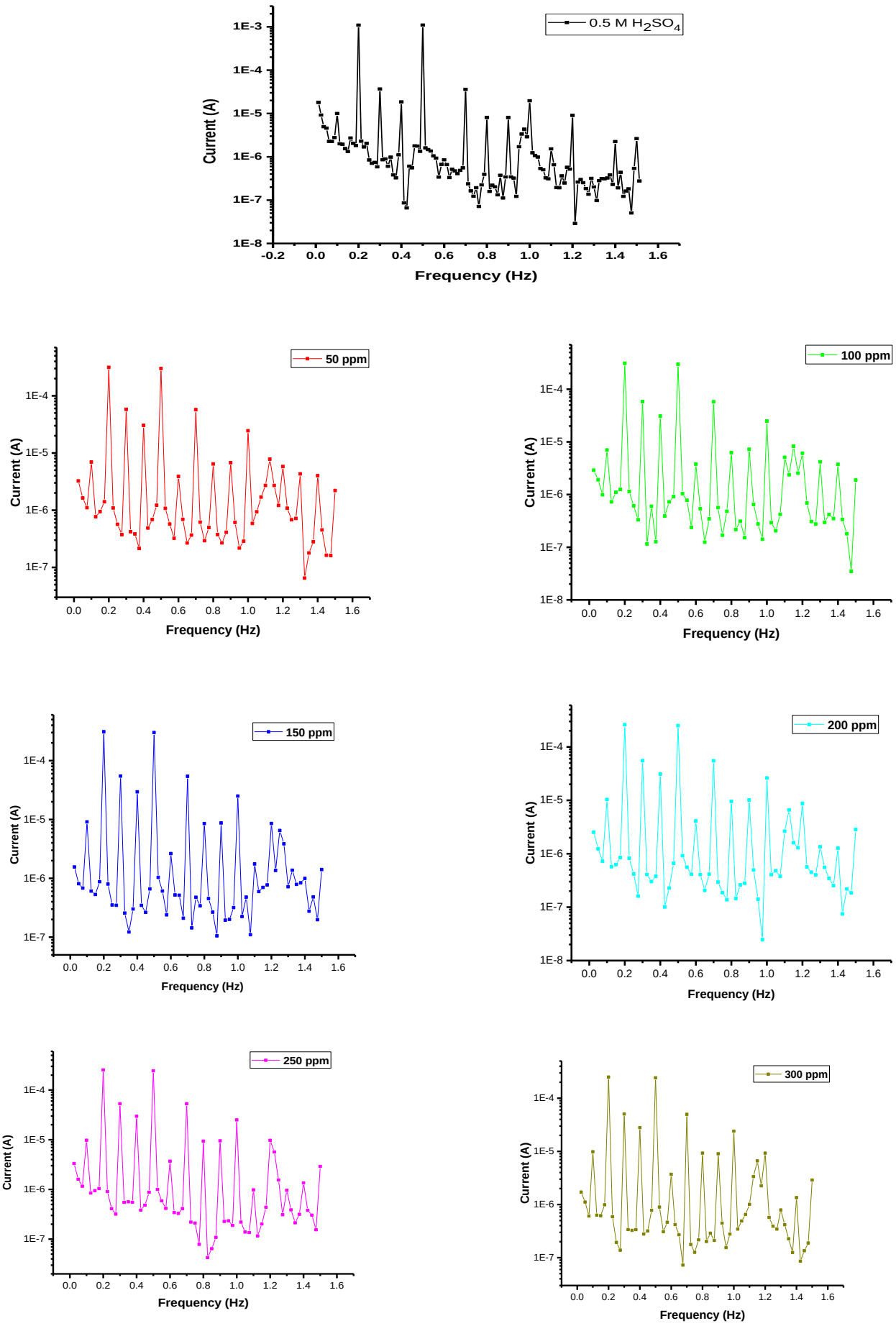

Figure 9. Intermodulation spectrum for CS in 0.5M H_2SO_4 for existence and nonexistence of unlike doses of Plantago major extract (50 – 300 ppm).

3.4.3. EFM tests.

The intermodulation spectra of CS were tested in 0.5 M H_2SO_4 in existence, and the nonexistence of diverse concentrations of Plantago major extract at 25°C was showed in Fig.9. The data of (i_{corr}, β_c, β_a, CF-2, CF-3, and %IE) obtained from EFM tests was shown in Table 6. The results proved that the i_{corr}, lowered by raising the dose of Plantago major extract while the efficiency of inhibitions (IE %) increasing. The causality factors obtained from tests are closed to theoretical values. The values of corrosion current densities can be obtained directly from EFM measurements and independent in Tafel constant. The IE % can be calculated as in Eq. (4). The values of (CF-2 and CF-3) attained are very close to the theoretical values (2 and 3), which revealed that the results are a really good quality [57].

Table 6. EFM for CS in the lack and existence of unlike concentrations of Plantago major extract at 25 ˚C.

Inh.	Conc. M	i_{corr}, µA cm^{-2}	β_c mV dec^{-1}	β_a mV dec^{-1}	CF-2	CF-3	K corr, mpy	θ	%IE
	0.5 M H_2SO_4	1750	152.4	116.3	1.91	4.06	1.01		
Plantago major	50	607.7	196.8	74.04	2.09	2.13	154.3	0.653	65.3
	100	591.1	186.3	72.80	2.08	2.83	150.0	0.662	66.2
	150	417.2	174.1	59.9	1.99	4.317	105.9	0.762	76.2
	200	314.4	171.1	52.4	1.92	2.88	79.8	0.820	82.0
	250	299.2	160.2	51.82	1.93	2.90	75.9	0.829	82.9
	300	290.0	148.2	51.90	1.94	2.83	73.7	0.834	83.4

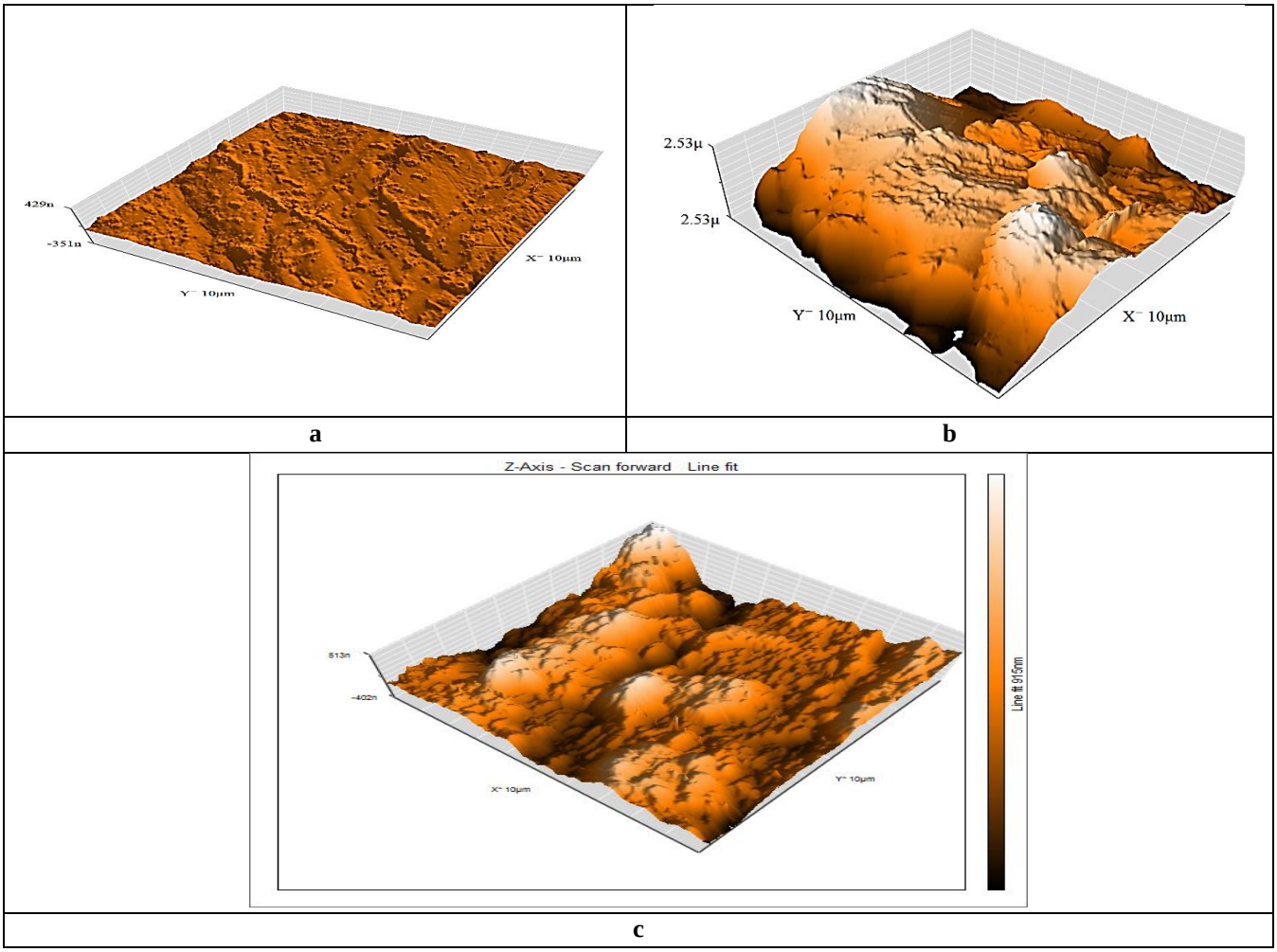

Figure 10. AFM images for CS (a) for pure surface, (b) after one-day immersion in 0.5 M H_2SO_4 solution, and (c) presence of 300 ppm Plantago major extract.

3.5. The surface examination by (AFM).

The surface morphology of CS was examined by AFM technique when immersed in a media of 0.5 M H_2SO_4 with and without 300 ppm of Plantago major extract and for pure CS sample after treatment by physical methods as ML measurements. Fig (10-a) showed the 3-D image for pure CS surface. Fig (10-b) showed the 3-D image for CS surface in 0.5 M H_2SO_4 for 24 hours. In this image, we can see that the surface was more corroded and destroyed compared to the smooth surface of pure CS. In the case of added 300 ppm of investigated extract, Fig (10-c) showed the 3-D image for the CS surface was less destroyed and became smoother than in the case of CS in corrosive media. The average roughness of the polished CS, CS surface in 0.5 M H_2SO_4 before and after adding the present inhibitor was measured to be 17.46 nm, 993.76 nm, and 165.8 nm, alternatively. The adsorption of Plantago major extract on the CS surface was evidenced by 3-D images and other results [58].

3.6. FT-IR characterization.

The IR spectra of pure Plantago major extract and layer produced on the CS surface immersed in 0.5 M H_2SO_4 treated with 300 ppm of Plantago major extract after 24 hours was shown in Fig. 11. From this figure, we can note that the IR spectra of Plantago major extract have the same characteristics as the IR spectra of the product created on the CS surface, indicating that the Plantago major extract is adsorbed on the CS surface. The IR spectra of the Plantago major extract showed that the band acquired at 3358 cm^{-1} could be corresponded to (OH). The peaks at 1648 cm^{-1} refer to (C=C), the one at 1408 cm^{-1} can be attributed to (S=O), and the frequency at 1011 cm^{-1} can be ascribed to (C-N). By comparing the spectra of the Plantago major pure extracts with that of the corrosion, the product also showed in Fig. 11. It is shown that there were shifted in the frequencies. The (O-H) stretched at 3358 cm^{-1} was moved to 3424 cm^{-1}, the C=C transferred at 1648 cm^{-1} was moved to 1635 cm^{-1}, the (S=O) stretched at 1408 cm^{-1} was moved to 1399 $cm^{-1,}$ and (C-N) stretched at 1011 cm^{-1} was moved to 1078 cm^{-1}. There interaction between the Plantago major extract and CS surface. The shifted in the spectra indicated that the interaction between Plantago major and CS happened due to the presence of functional groups in this extract.

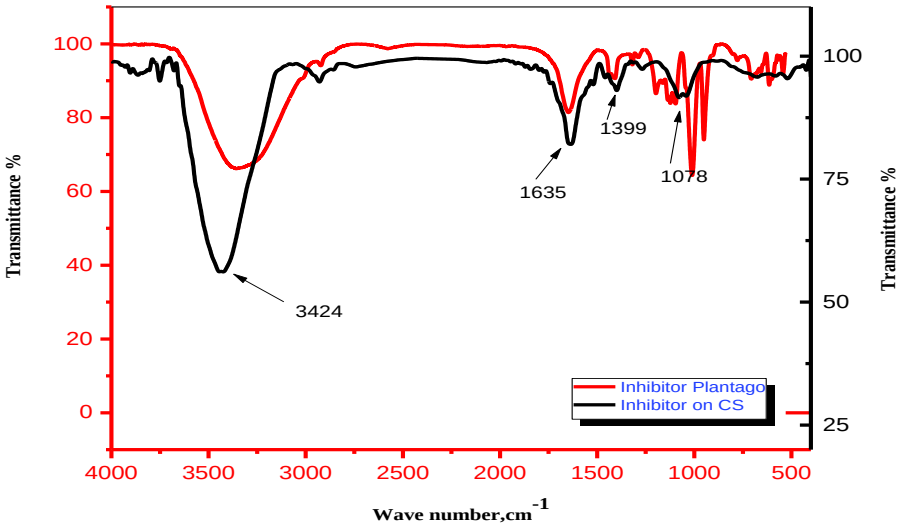

Figure 11. FT-IR spectra for inhibitor Plantago major adsorbed on CS surface at 25°C.

3.7. Inhibition mechanism.

The leaves of Plantago major plant mainly have alkaloids, terpenoids, phenolic acid derivatives, iridoid glycosides, flavonoids, and fatty acids. The adsorption of inhibitor on the CS surface by way of the chemisorption includes the movement of water molecules from the CS surface and donor-acceptor connections among empty d-orbitals of iron, π-electrons, and lone pairs of electrons presented in Plantago major constituents. In the acid medium, the steel surface bear's positive charge, so it is complicated for the protonated molecules to adsorb on the CS surface due to the electrostatic repulsion. Plantago major constituents have lone-pairs of electrons of O, S, N atoms and π-electrons of the aromatic rings, which may associate with vacant d-orbital of iron produced coordinate bond (chemisorption) creating a strongly protective adsorbed film on the CS surface. This interaction mode was in accord with the values of ΔG°_{ads}, where the adsorption of Plantago major constituents is chemisorption. By raising the temperature, the chemisorption is improved.

4. Conclusions

According to chemical, electrochemical measurements, and surface analysis, we can conclude that: Plantago major leaves extract good green and sustainable corrosion inhibitor for L80-carbon steel in 0.5 M H_2SO_4 solutions and considered as mixed type inhibitor as reported by PDP measurements; The inhibition efficiency of Plantago major extract was enhanced with increasing of both concentration and temperature as reported by ML measurements (94.9%); The adsorption of the Plantago major extract constituents on the surface of CS was endorsed by lowering the values of the double-layer capacitance (C_{dl}) comparison with a blank solution after the Plantago major extract are added. Moreover, this adsorption is affirmed by AFM and FT-IR analysis; The adsorption of Plantago major extract constituents on the surface of CS conforms with Temkin adsorption isotherm and is considered as chemisorption. Furthermore, by raising the temperature, chemisorption is improved based on the values of ΔG°_{ads}.

Funding

This research received no external funding.

Acknowledgments

This research has no acknowledgment.

Conflicts of Interest

The authors declare no conflict of interest.

References

1. Nazeera Banu, V.R.; Rajendran, S.; Senthil Kumaran, S. Investigation of the inhibitive effect of Tween 20 self assembling nanofilms on corrosion of carbon steel. *Journal of Alloys and Compounds* **2016**, *675*, 139-148, https://doi.org/10.1016/j.jallcom.2016.02.247.
2. Haldhar, R.; Prasad, D.; Bahadur, I.; Dagdag, O.; Berisha, A. Evaluation of Gloriosa superba seeds extract as corrosion inhibition for low carbon steel in sulfuric acidic medium: A combined experimental and computational studies. *Journal of Molecular Liquids* **2021**, *323*, https://doi.org/10.1016/j.molliq.2020.114958.

3. Pal, A.; Das, C. A novel use of solid waste extract from tea factory as corrosion inhibitor in acidic media on boiler quality steel. *Industrial Crops and Products* **2020**, *151*, https://doi.org/10.1016/j.indcrop.2020.112468.
4. Hamilton-Amachree, A.; Iroha, N. Corrosion inhibition of API 5L X80 pipeline steel in acidic environment using aqueous extract of Thevetia peruviana. *Chemistry International* **2019**, *6*, 117-128, https://doi.org/10.5281/zenodo.3516565.
5. Yüce, A.O. Corrosion Inhibition Behavior of Robinia pseudoacacia Leaves Extract as a Eco-Friendly Inhibitor on Mild Steel in Acidic Media. *Metals and Materials International* **2020**, *26*, 456-466, https://doi.org/10.1007/s12540-019-00509-7.
6. Benarioua, M.; Mihi, A.; Bouzeghaia, N.; Naoun, M. Mild steel corrosion inhibition by Parsley (Petroselium Sativum) extract in acidic media. *Egyptian Journal of Petroleum* **2019**, *28*, 155-159, https://doi.org/10.1016/j.ejpe.2019.01.001.
7. Abdallah, M.; Altass, H.M.; Al Jahdaly, B.A.; Salem, M.M. Some natural aqueous extracts of plants as green inhibitor for carbon steel corrosion in 0.5 M sulfuric acid. *Green Chemistry Letters and Reviews* **2018**, *11*, 189-196, https://doi.org/10.1080/17518253.2018.1458161.
8. Elabbasy, H.M.; Zidan, S.M., El-Aziz, A.F.S. Inhibitive behavior of Ambrosia Maritima extract as an eco-friendly corrosion inhibitor for carbon steel in 1M HCI. *Zaštita materijala* **2019,** *60*, 129-146, https://doi.org/10.5937/zasmat1902129E.
9. Elabbasy, H.M.; Fouda, A.S. Olive leaf as green corrosion inhibitor for C-steel in Sulfamic acid solution. *Green Chemistry Letters and Reviews* **2019**, *12*, 332-342, https://doi.org/10.1080/17518253.2019.1646812.
10. Fouda, A.E.-A.S.; Eissa, M. Adenium obesum Extract as a Safe Corrosion Inhibitor for C-Steel in NaCl Solutions: Investigation of Biological Effects. *Journal of Bio- and Tribo-Corrosion* **2020**, *6*, 1-11, https://doi.org/10.1007/s40735-020-00394-3.
11. Fouda, A.S.; Abdel Haleem, E. Berry Leaves Extract as Green Effective Corrosion Inhibitor for Cu in Nitric Acid Solutions. *Surface Engineering and Applied Electrochemistry* **2018**, *54*, 498-507, https://doi.org/10.3103/S1068375518050034.
12. Tezeghdenti, M.; Dhouibi, L.; Etteyeb, N. Corrosion Inhibition of Carbon Steel in 1 M Sulphuric Acid Solution by Extract of Eucalyptus globulus Leaves Cultivated in Tunisia Arid Zones. *Journal of Bio- and Tribo-Corrosion* **2015**, *1*, https://doi.org/10.1007/s40735-015-0016-x.
13. Fouda, A.S.; Abd El-Maksoud, S.A.; Belal, A.A.M.; El-Hossiany, A.; Ibrahium, A. Effectiveness of Some Organic Compounds as Corrosion Inhibitors for Stainless Steel 201 in 1M HCl: Experimental and Theoretical Studies. *Int. J. Electrochem. Sci* **2018**, *13*, 9826-9846, https://doi.org/10.20964/2018.10.36.
14. Fouda, A.S.; Ibrahim, H.; Rashwaan, S.; El-Hossiany, A.; Ahmed, R.M. Expired Drug (pantoprazole sodium) as a Corrosion Inhibitor for High Carbon Steel in Hydrochloric Acid Solution. *International Journal of Electrochemical Science* **2018**, *13*, 6327-6346, https://doi.org/10.20964/2018.07.33.
15. Fouda, A.E.A.S.; Rashwan, S.M.; Kamel, M.M.; Haleem, E.A. Juglans Regia Extract (JRE) as Eco-Friendly Inhibitor for Aluminum Metal in Hydrochloric Acid Medium. *Biointerface Research in Applied Chemistry* **2020**, *10*, https://doi.org/10.33263/BRIAC105.63986416.
16. Fouda, A.S.; Shalabi, K.; Nofal, A.M.; Elzekred, M. Methanol Extract of Rumex Vesicarius L. as Eco-Friendly Corrosion Inhibitor for Carbon Steel in Sulfuric Acid Solution. *Chemical Science Transactions* **2018**, *7*, 101-111, https://doi.org/10.7598/cst2018.1430.
17. Yang, J.; Lu, Y.; Guo, Z.; Gu, J.; Gu, C. Corrosion behaviour of a quenched and partitioned medium carbon steel in 3.5wt.% NaCl solution. *Corrosion Science* **2018**, *130*, 64-75, https://doi.org/10.1016/j.corsci.2017.10.027.
18. Essien, E.A.; Kavaz, D.; Ituen, E.B.; Umoren, S.A. Synthesis, characterization and anticorrosion property of olive leaves extract-titanium nanoparticles composite. *Journal of Adhesion Science and Technology* **2018**, *32*, 1773-1794, https://doi.org/10.1080/01694243.2018.1445800.
19. Almzarzie, K.; Falah, A.; Massri, A.; Kellawi, H. Electrochemical Impedance Spectroscopy (EIS) and Study of Iron Corrosion Inhibition by Turmeric Roots Extract (TRE) in Hydrochloric Acid Solution. *Egyptian Journal of Chemistry* **2019**, *62*, 501-512, https://dx.doi.org/10.21608/ejchem.2018.5295.1476.
20. Alvarez, P.E.; Fiori-Bimbi, M.V.; Neske, A.; Brandán, S.A.; Gervasi, C.A. Rollinia occidentalis extract as green corrosion inhibitor for carbon steel in HCl solution. *Journal of Industrial and Engineering Chemistry* **2018**, *58*, 92-99, https://doi.org/10.1016/j.jiec.2017.09.012.
21. Boucherit, L.; Douadi, T.; Chafai, N.; Al-Noaimi, M.; Chafaa, S. The inhibition Activity of 1,10 - bis(2-formylphenyl)-1,4,7,10- tetraoxadecane (Ald) and its Schiff base (L) on the Corrosion of Carbon Steel in HCl: Experimental and Theoretical Studies. *International journal of electrochemical science* **2018**, *13*, 3997-4025, https://doi.org/10.20964/2018.04.59.
22. Abd El-Lateef, H.M.; Abu-Dief, A.M.; Mohamed, M.A.A. Corrosion inhibition of carbon steel pipelines by some novel Schiff base compounds during acidizing treatment of oil wells studied by electrochemical and quantum chemical methods. *Journal of Molecular Structure* **2017**, *1130*, 522-542, https://doi.org/10.1016/j.molstruc.2016.10.078.
23. Debab, H.; Douadi, T.; Djamel, D.; Issaadi, S.; Chafaa, S. Electrochemical and Quantum Chemical Studies of Adsorption and Corrosion Inhibition of Two New Schiff Bases on Carbon Steel in Hydrochloric Acid

Media. *International journal of electrochemical science* **2018**, *13*, 6958-6977, https://doi.org/10.20964/2018.07.19.
24. Benabbouha, T.; Siniti, M.; El Attari, H.; Chefira, K.; Chibi, F.; Nmila, R.; Rchid, H. Red Algae Halopitys Incurvus Extract as a Green Corrosion Inhibitor of Carbon Steel in Hydrochloric Acid. *Journal of Bio- and Tribo-Corrosion* **2018**, *4*, https://doi.org/10.1007/s40735-018-0161-0.
25. Addi, B.; Addi, A.; Shaban, A.; Habib, E.; Ait Addi, E.H.; Hamdani, M. Tin corrosion inhibition by molybdate ions in 0.2 M maleic acid solution: Electrochemical and surface analytical study. *Mediterranean Journal of Chemistry* **2020**, *10*, 465-476, http://dx.doi.org/10.13171/mjc019.
26. Adom, M.B.; Taher, M.; Mutalabisin, M.F.; Amri, M.S.; Abdul Kudos, M.B.; Wan Sulaiman, M.W.A.; Sengupta, P.; Susanti, D. Chemical constituents and medical benefits of Plantago major. *Biomedicine & Pharmacotherapy* **2017**, *96*, 348-360, https://doi.org/10.1016/j.biopha.2017.09.152.
27. Zubair, M.; Widén, C.; Renvert, S.; Rumpunen, K. Water and ethanol extracts of Plantago major leaves show anti-inflammatory activity on oral epithelial cells. *Journal of Traditional and Complementary Medicine* **2019**, *9*, 169-171, https://doi.org/10.1016/j.jtcme.2017.09.002.
28. Mukemre, M.; Konczak, I.; Uzun, Y.; Dalar, A. Phytochemical profile and biological activities of Anatolian Plantain (Plantago anatolica). *Food Bioscience* **2020**, *36*, https://doi.org/10.1016/j.fbio.2020.100658.
29. Genc, Y.; Dereli, F.T.G.; Saracoglu, I.; Akkol, E.K. The inhibitory effects of isolated constituents from Plantago major subsp. major L. on collagenase, elastase and hyaluronidase enzymes: Potential wound healer. *Saudi Pharmaceutical Journal* **2020**, *28*, 101-106, https://doi.org/10.1016/j.jsps.2019.11.011.
30. Fernandes, C.M.; Ferreira Fagundes, T.d.S.; Escarpini dos Santos, N.; Shewry de M. Rocha, T.; Garrett, R.; Borges, R.M.; Muricy, G.; Valverde, A.L.; Ponzio, E.A. Ircinia strobilina crude extract as corrosion inhibitor for mild steel in acid medium. *Electrochimica Acta* **2019**, *312*, 137-148, https://doi.org/10.1016/j.electacta.2019.04.148.
31. Fouda, A.S.; Abousalem, A.S.; El-Ewady, G.Y. Mitigation of corrosion of carbon steel in acidic solutions using an aqueous extract of Tilia cordata as green corrosion inhibitor. *International Journal of Industrial Chemistry* **2017**, *8*, 61-73, https://doi.org/10.1007/s40090-016-0102-z.
32. Saraswat, V.; Yadav, M. Computational and electrochemical analysis on quinoxalines as corrosion inhibitors for mild steel in acidic medium. *Journal of Molecular Liquids* **2020**, *297*, https://doi.org/10.1016/j.molliq.2019.111883.
33. Ouakki, M.; Galai, M.; Rbaa, M.; Abousalem, A.S.; Lakhrissi, B.; Touhami, M.E.; Cherkaoui, M. Electrochemical, thermodynamic and theoretical studies of some imidazole derivatives compounds as acid corrosion inhibitors for mild steel. *Journal of Molecular Liquids* **2020**, *319*, https://doi.org/10.1016/j.molliq.2020.114063.
34. Al-Nami, S. Corrosion Inhibition Effect and Adsorption Activities of methanolic myrrh extract for Cu in 2 M HNO3. *International Journal of Electrochemical Science* **2020**, *15*, 1187-1205, https://doi.org/10.20964/2020.02.23.
35. Fouda, A.S.; El-Ewady, G.; Ali, A.H. Modazar as promising corrosion inhibitor of carbon steel in hydrochloric acid solution. *Green Chemistry Letters and Reviews* **2017**, *10*, 88-100, https://doi.org/10.1080/17518253.2017.1299228.
36. Asfia, M.P.; Rezaei, M.; Bahlakeh, G. Corrosion prevention of AISI 304 stainless steel in hydrochloric acid medium using garlic extract as a green corrosion inhibitor: Electrochemical and theoretical studies. *Journal of Molecular Liquids* **2020**, *315*, https://doi.org/10.1016/j.molliq.2020.113679.
37. Saeed, M.T.; Saleem, M.; Usmani, S.; Malik, I.A.; Al-Shammari, F.A.; Deen, K.M. Corrosion inhibition of mild steel in 1 M HCl by sweet melon peel extract. *Journal of King Saud University - Science* **2019**, *31*, 1344-1351, https://doi.org/10.1016/j.jksus.2019.01.013.
38. El-Aziz, E.S.F.A.; Mahmoud, R.S.; Ibrahim, H.; Ezzat, A.R. Expired nizatidine drug as eco-friendly corrosion Inhibitor for alpha-brass alloy in aqueous solutions. Zaštita materijala **2020**, *61*, 192-209, https://doi.org/10.5937/zasmat2003192F.
39. Aslam, J.; Aslam, R.; Lone, I.H.; Radwan, N.R.; Mobin, M.; Aslam, A.; Alzulaibani, A.A. Inhibitory effect of 2-Nitroacridone on corrosion of low carbon steel in 1 M HCl solution: An experimental and theoretical approach. *Journal of Materials Research and Technology* **2020,** *9*, 4061-4075, https://doi.org/10.1016/j.jmrt.2020.02.033.
40. Kumar, P.R.A.D.E.E.P.; Kalia, V.I.K.A.S.; Kumar, H.A.R.I.S.H.; Dahiya, H.A.R.I.O.M. Corrosion Inhibition for Mild Steel in Acidic Medium by Using Hexadecylamine as Corrosion Inhibitor. *Chem. Sci. Trans* **2017**, *6*, 497–512, https://doi.org/10.7598/cst2017.1421.
41. Abd El Rehim, S.S.; Hassan, H.H.; Amin, M.A. Corrosion inhibition of aluminum by 1,1(lauryl amido)propyl ammonium chloride in HCl solution. *Materials Chemistry and Physics* **2001**, *70*, 64-72, https://doi.org/10.1016/S0254-0584(00)00468-5.
42. Tang, L.; Li, X.; Si, Y.; Mu, G.; Liu, G. The synergistic inhibition between 8-hydroxyquinoline and chloride ion for the corrosion of cold rolled steel in 0.5M sulfuric acid. *Materials Chemistry and Physics* **2006**, *95*, 29-38, https://doi.org/10.1016/j.matchemphys.2005.03.064.
43. Putilova, I.N.; Balezin, S.A.; Barannik, V.P. Metallic corrosion inhibitors. *Pergamon Press. J. Electrochem. Soc.* **1960**, *108*.

44. Salhi, A.; Tighadouini, S.; El-Massaoudi, M.; Elbelghiti, M.; Bouyanzer, A.; Radi, S.; El Barkany, S.; Bentiss, F.; Zarrouk, A. Keto-enol heterocycles as new compounds of corrosion inhibitors for carbon steel in 1M HCl: Weight loss, electrochemical and quantum chemical investigation. *Journal of Molecular Liquids* **2017**, *248*, 340-349, https://doi.org/10.1016/j.molliq.2017.10.040.
45. Yadav, M.; Sarkar, T.K.; Obot, I.B. WITHDRAWN: Indolines as novel corrosion inhibitors: Electrochemical, XPS, DFT and molecular dynamics simulation studies. *Corrosion Science* **2017**, https://doi.org/10.1016/j.corsci.2017.03.002.
46. Yadav, M.; Sinha, R.R.; Sarkar, T.K.; Bahadur, I.; Ebenso, E.E. Application of new isonicotinamides as a corrosion inhibitor on mild steel in acidic medium: Electrochemical, SEM, EDX, AFM and DFT investigations. *Journal of Molecular Liquids* **2015**, *212*, 686-698, https://doi.org/10.1016/j.molliq.2015.09.047.
47. Maridevarmath, C.V.; Malimath, G.H. Studies on the effect of temperature on dielectric relaxation, activation energy (ΔG*), enthalpy (ΔH*), entropy (ΔS*) and molecular interactions of some anilines, phenol and their binary mixtures using X-band microwave bench. *The Journal of Chemical Thermodynamics* **2020**, *144*, https://doi.org/10.1016/j.jct.2020.106068.
48. Umoren, S.A.; Inam, E.I.; Udoidiong, A.A.; Obot, I.B.; Eduok, U.M.; Kim, K.-W. Humic Acid from Livestock Dung: Ecofriendly Corrosion Inhibitor for 3SR Aluminum Alloy in Alkaline Medium. *Chemical Engineering Communications* **2015**, *202*, 206-216, https://doi.org/10.1080/00986445.2013.836635.
49. Zhu, H.; Huo, Y.; Wang, W.; He, X.; Fang, S.; Zhang, Y. Quantum chemical calculation of reaction characteristics of hydroxyl at different positions during coal spontaneous combustion. *Process Safety and Environmental Protection* **2021**, *148*, 624-635, https://doi.org/10.1016/j.psep.2020.11.041.
50. Unnisa, C.B.N.; Chitra, S.; Nirmala Devi, G.; Kiruthika, A.; Roopan, S.M.; Hemapriya, V.; Chung, I.-M.; Kim, S.-H.; Prabakaran, M. Electrochemical and nonelectrochemical analyses of cardo polyesters at the metal/0.5 M H2SO4 interface for corrosion protection. *Research on Chemical Intermediates* **2019**, *45*, 5425-5449, https://doi.org/10.1007/s11164-019-03910-4.
51. Shalabi, K.; Helmy, A.M.; El-Askalany, A.H.; Shahba, M.M. New pyridinium bromide mono-cationic surfactant as corrosion inhibitor for carbon steel during chemical cleaning: Experimental and theoretical studies. *Journal of Molecular Liquids* **2019**, *293*, https://doi.org/10.1016/j.molliq.2019.111480.
52. Eid, A.M.; Shaaban, S.; Shalabi, K. Tetrazole-based organoselenium bi-functionalized corrosion inhibitors during oil well acidizing: Experimental, computational studies, and SRB bioassay. *Journal of Molecular Liquids* **2020**, *298*, https://doi.org/10.1016/j.molliq.2019.111980.
53. Sığırcık, G.; Yildirim, D.; Tüken, T. Synthesis and inhibitory effect of N,N'-bis(1-phenylethanol)ethylenediamine against steel corrosion in HCl Media. *Corrosion Science* **2017**, *120*, 184-193, https://doi.org/10.1016/j.corsci.2017.03.003.
54. Shalabi, K.; Nazeer, A.A. Ethoxylates nonionic surfactants as promising environmentally safe inhibitors for corrosion protection of reinforcing steel in 3.5 % NaCl saturated with Ca(OH)2 solution. *Journal of Molecular Structure* **2019**, *1195*, 863-876, https://doi.org/10.1016/j.molstruc.2019.06.033.
55. Abdallah, Y.M.; Shalabi, K.; Bayoumy, N.M. Eco-friendly synthesis, biological activity and evaluation of some new pyridopyrimidinone derivatives as corrosion inhibitors for API 5L X52 carbon steel in 5% sulfamic acid medium. *Journal of Molecular Structure* **2018**, *1171*, 658-671, https://doi.org/10.1016/j.molstruc.2018.06.045.
56. Ituen, E.; Akaranta, O.; James, A.; Sun, S. Green and sustainable local biomaterials for oilfield chemicals: Griffonia simplicifolia extract as steel corrosion inhibitor in hydrochloric acid. *Sustainable Materials and Technologies* **2017**, *11*, 12-18, https://doi.org/10.1016/j.susmat.2016.12.001.
57. Mobin, M.; Zehra, S.; Parveen, M. l-Cysteine as corrosion inhibitor for mild steel in 1M HCl and synergistic effect of anionic, cationic and non-ionic surfactants. *Journal of Molecular Liquids* **2016**, *216*, 598-607, https://doi.org/10.1016/j.molliq.2016.01.087.